JACS
JOURNAL OF THE AMERICAN CHEMICAL SOCIETY
Cite This: J. Am. Chem. Soc. 2018, 140, 2756−2760
Communication
pubs.acs.org/JACS

Charge-Transfer within Zr-Based Metal−Organic Framework: The Role of Polar Node

Andrea Van Wyk,[†,§] Tanner Smith,[†] Jaehong Park,[‡] and Pravas Deria*[,†]

[†]Department of Chemistry and Biochemistry, Southern Illinois University, 1245 Lincoln Drive, Carbondale, Illinois 62901, United States

[‡]Department of Molecular Engineering, Kyoto University, Katsura, Nishikyo-ku, Kyoto 615-8510, Japan

Supporting Information

ABSTRACT: Metal−organic frameworks (MOFs) are emerging materials for electro- and photo-chemical applications, where an understanding of the underlying charge-transfer (CT) process will facilitate designing new materials. However, the involvement of counterions in traditional electrochemical experiments complicates the probe on the role of various components during a CT event. A CT reaction between photoexcited MOF linker and a node−anchored ferrocene, within mesoporous framework NU-1000, was spectroscopically probed without the involvement of electrolyte based counterions. Dielectric dependent CT kinetics indicate that the process involves a high reorganization energy that is required to polarize the node bound hydroxyl/aqua ligands. The findings have clear implication on the design of MOF-based electrocatalysis and photoelectrochemical devices.

Metal−organic frameworks (MOFs)[1] are emerging porous molecular compositions for optoelectronic applications[2] owing to their modular structures. Diversity in their chemical structure highlights an enormous range of pore size and geometry stemming from a wide variety of topological networks constructed with multitopic linkers and metal-based nodes.[1b,3] Structures assembled from photo[2f,h,4] and redox[5] active building blocks, as well as various postsynthesis techniques[6] that enable installation of supportive chemical functionality,[7] can facilitate these crystalline compositions for light harvesting (LH),[8] energy conversion,[5e,9] and storage[10] systems.

Though light harvesting requires efficient and directional energy transfer, photon energy conversion requires an electron transfer process within the framework.[11] Likewise, electrocatalytic[5e,9] and energy storage[10] applications require an efficient charge transport process.[12] Literature reports[5f,12] suggest that the energy mismatch between the linkers and metal-oxo nodes enforces a charge hopping for the transport processes, where a counterion is coupled with the redox processes of the linkers. Involvement of the counterion alters the charge-transfer (CT) kinetics by modifying the driving force [e.g., $L^+-PF_6^- + L^0 \rightarrow L^0 + L^+-PF_6^-$] and activation energy relative to the case where no counterion is involved [i.e., $L^+ + L^0 \rightarrow L^0 + L^+$] and thus making the charge transport process asymmetric.[12]

As counterion migration accompanies an electrochemical CT reaction within the narrow pores, it can potentially lead to unique situations including a slower kinetic and selective redox reaction.[5f,12,13] To decouple the effect of counterions delivered by the electrolyte solution and understand the charge transport process within the narrow pores of the crystalline materials, we chose to study the CT quenching process of a photoexcited linker. Given that Zr^{IV}−based MOFs[2j,6c,14] provide robust materials that are amenable to postsynthetic functionalization,[5f,g,7a,c,d,15] we used a well-established pyrene-based MOF NU-1000 featuring the deprotonated form of 1,3,6,8-tetrakis(*p*-benzoicacid)pyrene (H_4TBAPy) and $[Zr_6(\mu_3-O)_4(\mu_3-OH)_4(-OH)_4(-OH_2)_4]^{8+}$ nodes.[6c] Microcrystalline NU-1000 samples were decorated with ferrocene carboxylate via a SALI-based node functionalization technique (Figure 1) generating **Fc@NU-1000**.[5f,7,13]

Figure 1b,c highlights the DFT-optimized structure where the ferrocene moiety is rigidly anchored to the node at a close proximity to the Zr^{IV}-oxo cluster; the phenyl-arms of the adjacent TBAPy linkers restrict its rotational flexibility to define

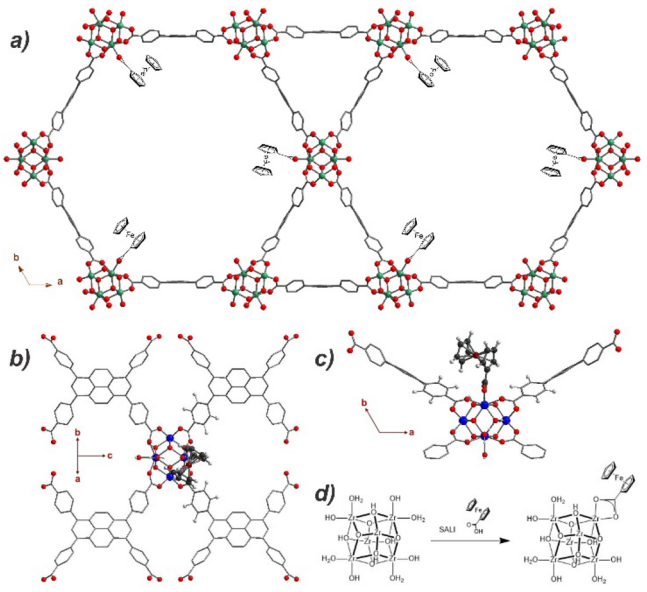

Figure 1. (a) Structure of the **Fc@NU-1000**; (b, c) DFT optimized partial structures highlighting the "rigidly" bound ferrocene moiety at the Zr^{IV}-oxo node; (d) SALI functionalization method.

Received: December 14, 2017
Published: February 9, 2018

DOI: 10.1021/jacs.7b13211
J. Am. Chem. Soc. 2018, 140, 2756−2760

a "fixed" donor−acceptor system. This computational model suggests a Fc-to-nearest TBAPy (center-to-center) distance of 9.7 Å (see SI Sec C). Electrochemical data (Figure 2) indicate

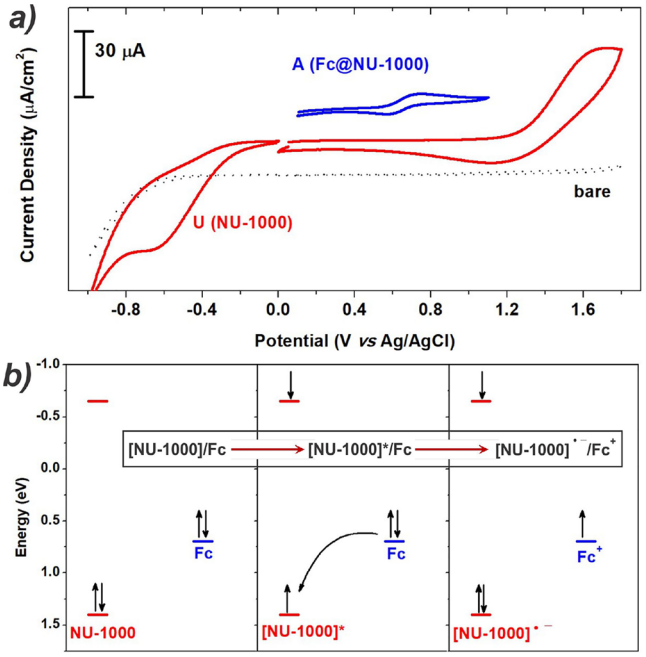

Figure 2. (a) Cyclic voltammograms of NU-1000 and **Fc@NU-1000**. Experimental condition: sample deposited on FTO electrode (1.2 cm^2), 0.1 M $TBAPF_6$ in acetonitrile, scan rate is 50 mV/s. (b) Corresponding energy diagram showing photoexcited charge-transfer process in **Fc@NU-1000** sample.

that the anchored ferrocene moiety in **Fc@NU-1000** features a Fc/Fc^+ redox potential of +0.7 V, where the TBAPy in unmodified NU-1000 can be electrochemically oxidized at +1.4 V (vs Ag/AgCl).[5f,13] These electrochemical data suggest that the excited-state reduction potential of the TBAPy ($^1E^{-/*}$ = +1.4 V) lies 700 mV more positive than the Fc/Fc^+ potential. Thus, a node-bound Fc moiety in **Fc@NU-1000** system can act as an electron donor to a photoexcited NU-1000* (or TBAPy*) acting as an electron acceptor. Because the pendant Fc-moiety in **FC@NU-1000** protrudes toward the mesopore (d ~ 30 Å; Figure 1), this composition represents an ideal system to study the effect of solvent dielectrics in the CT process within the MOF.

To verify that the [NU-1000]*/Fc can produce a photo-induced CT complex as predicted, excited-state dynamics of **Fc@NU-1000** samples were examined using femtosecond transient absorption (fs-TA) spectroscopy upon the photo-excitation (λ_{ex}) at 400 nm that predominantly excites NU-1000. Figure 3 highlights, in the early time (~0.6 ps, black), an intense NIR singlet excited-state absorption (ESA) band (~730 nm) and a corresponding bleaching band (500 nm) appear for the **Fc@NU-1000** sample. These transient spectroscopic features are reminiscent to the unmodified NU-1000 (Figure S4). However, with the decay of the S_1 (at 730 nm; τ ~ 15 ps), the **Fc@NU-1000** sample renders evolution of a new ESA peak at 600 nm with a sizable corresponding bleaching intensity at 500 nm, confirming the ESA feature at 600 nm is indeed a TBAPy-based species (τ_{delay} = 56 ps, green in Figure 3). As expected, this 600 nm ESA band is absent in pristine NU-1000 and matches to the spectral signature of the $TBAPy^{\bullet-}$ species

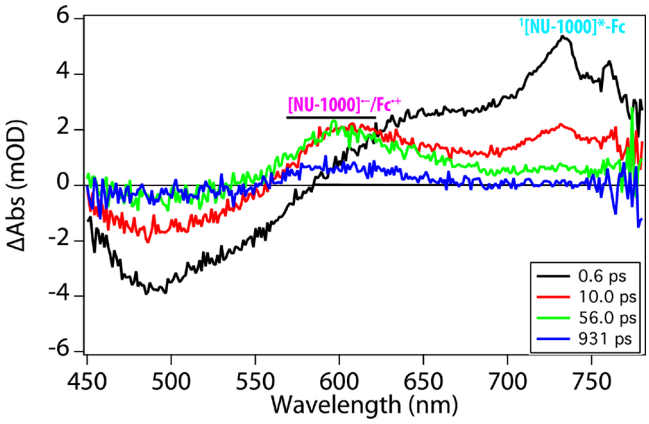

Figure 3. Representative fs-TA spectra of **Fc@NU-1000** in N_2 purged toluene solvent at the delay times noted. Experimental condition: λ_{ex} = 400 nm; excitation fluence = ~0.1 mJ/cm^2; Fc/TBAPy = 0.175.

(Figures S3, S4). Thus, we assign the transient feature at 600 nm as $[NU\text{-}1000]^{\bullet-}$ stemming from the [NU-1000]*/Fc species. The charge separation (CS) and thermal recombination (estimated from the rise and decay time constant of 600 nm ESA band) commence over *ca.* 9 and 430 ps time scale, respectively.

Because the signature peak for the charge-transferred product $[NU\text{-}1000]^{\bullet-}$ appears at 600 nm where the ESA band for [NU-1000]*/Fc species starts, we anticipated a possible complication in the analyses of the early time dynamical data. Thus, we used a classic fluorescence quenching experiment to study the CT process within this system. To do so, we first functionalized the Zr^{IV}-oxo nodes with varying degree of ferrocene-carboxylate ($Fc\text{-}COO^-$) by using a well-established SALI method.[5f,7a,c,13] Note that NU-1000 features a 8-connected node that can accommodate a maximum of four incoming $Fc\text{-}COO^-$ ligands (Fc/TBAPy = 2). However, for this study the range of installed $Fc\text{-}COO^-$ ligands was varied from zero to a maximum of 0.353 per TBAPy linker (0.000 (**U**), 0.006 (**F**), 0.015 (**E**), 0.030 (**D**), 0.093 (**C**), 0.175 (**B**), and 0.353 (**A**)) as determined via SEM-EDS method (see SI Sec C). These **Fc@NU-1000** samples were degassed and filled with nitrogen or nitrogen purged solvent. Steady-state emissive data (Figures 4 and S6) underscore a monotonic decrease in the emission intensity associated with the increase in the ferrocene loading. Excitation−emission mapping data suggest no spectral shift of the emission peak involved with the variation of the ferrocene loading.

Absolute quantum yield quickly diminishes with increasing ferrocene loading and plateaus at a Fc/TBAPy ratio of as low as ~0.06 (see Table S2; Figure S5). The saturation in the experimentally measured absolute quantum yield (Φ) is shown in Figure 5a as a plot of Φ/Φ_0 against the Fc/TBAPy ratio in various dielectric media (Φ_0, is the quantum yield of pristine NU-1000). Because excitons in MOF migrate through a fluorescence resonance energy transfer (FRET) process, an amplified quenching is observed.[17] The phenomena can be described as two competitive processes, where the photoexcited S_1 state depletes via a $S_1 \rightarrow S_0$ decay (emission) and CT reaction with ferrocene (quenching).[2h]

Transient emission decay profiles of these samples, in various solvents, indicate a faster decay profile with an increase in Fc/TBAPy ratio (Figures 5b, S7). From the saturation behavior of the emission quenching and the corresponding fluorescence

DOI: 10.1021/jacs.7b13211
J. Am. Chem. Soc. 2018, 140, 2756−2760

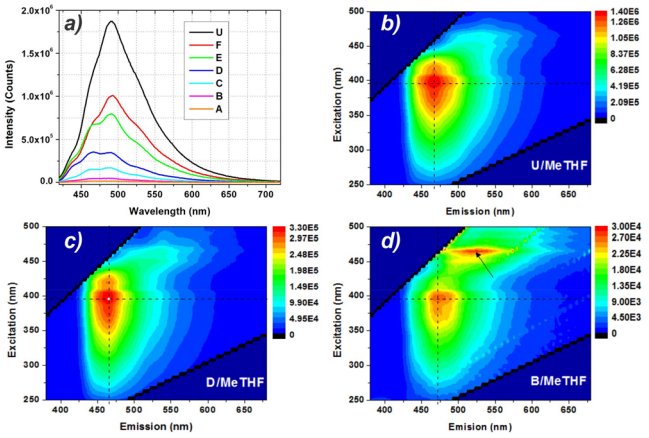

Figure 4. (a) Emission quenching as a function of Fc/TBAPy ratio; and (b–d) excitation–emission maps highlighting the transition energy. The arrow in panel (d) denotes residual low energy emission from a small amount of NU-901 impurity.[16] Experimental condition: solvent = 2-methyl tetrahydrofuran; T = 298 K.

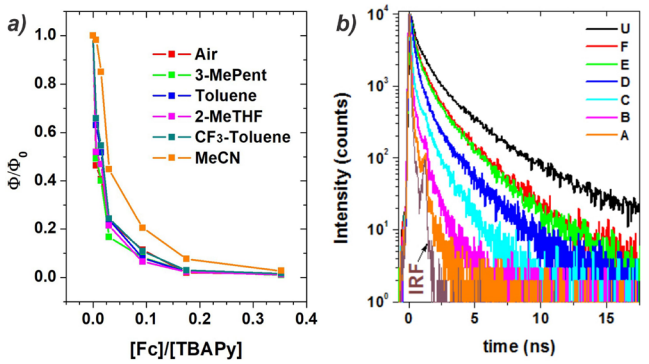

Figure 5. Emission quenching in **Fc@NU-1000**: (a) quenching efficiency and (b) transient emission decay profiles (in 2-methyl tetrahydrofuran solvent) highlighting fast decay with increase in Fc/TBAPy ratio.

lifetime data (Figures 5, S7 and Table SI-3), the CT rates were estimated from

$$\frac{\Phi_0}{\Phi_s} = 1 + \tau_0 k_e \tag{1}$$

where Φ_0 and τ_0 are the intrinsic fluorescence quantum yield and lifetime without quenchers, respectively; Φ_s is the saturated fluorescence quantum yield; and k_e is the CT (quenching) rate.

The CT time constant obtained from the emission quenching experiment is consistent with the fs-transient spectroscopic data. For example, in toluene solvent, the CT time constants are 13 and 9 ps from the emission quenching and fs-data, respectively. Furthermore, considering the distance between the Fc and its closest TBAPy linker, these rate constants are within the range predicted in literature for r_{DA} ≃10 Å.[19] In absence of ferrocene-carboxylates or TBAPy compounds with varying oxidation potentials, we sought to analyze the CT rates as a function of solvent dielectrics. Our experimental rate constant values (Table 1) vary only by a factor of 3 in response to a dielectric variation of 37. This nonresponsive kinetics indicate that this system possesses high total reorganization energy comparable to the CT driving force. The estimated ΔG^0 value, using the standard Weller equation,[20] was found to be −0.739 eV in acetonitrile solvent and will

Table 1. Charge-Transfer Parameters in FC@NU-1000

Media	ϵ_s	$k_e \times 10^{10}$ (s^{-1})	λ_s (eV)[a]
Air	1.0006	9.4	0
3-MePent	1.89	8.6	0
Toluene	2.38	7.5	0.041
2-MeTHF	6.97	7.4	0.576
CF_3-Toluene	9.18	6.7	0.621
MeCN	37	2.8	0.837

[a]The solvent reorganization energy (λ_s) for the bulk solvent was calculated by the Marcus relation (eq below).[18] $\lambda_s = \frac{e^2}{4\pi\epsilon_0}\left(\frac{1}{2r_D} + \frac{1}{2r_A} - \frac{1}{r_{DA}}\right)\left(\frac{1}{n^2} - \frac{1}{\epsilon_s}\right)$ Where ϵ_0 is the permittivity of free space, ϵ_s the static dielectric constant of the solvent, n is the refractive index, and e the magnitude of the charge of an electron; r_{DA} the center-to-center distance between Fc and the closest TBAPy, measured from the DFT optimized structure (10 Å; Figure 1), r_D the effective radius of the donor ion (3.5 Å), and r_A the effective radius of the acceptor ion (7.4 Å).]

slightly increase in low dielectric media (−1.085 eV for dry sample; assuming a fixed donor–acceptor size and distance). We know, from the Marcus theory[21] that the reorganization energy plays a crucial role in CT rate kinetics process.

$$k_e = \frac{2\pi}{\hbar} H_{DA}{}^2 \frac{1}{\sqrt{4\pi\lambda_t k_b T}} \exp\left[-\frac{(\lambda_t + \Delta G^0)^2}{4\pi\lambda_t k_b T}\right] \tag{2}$$

Where H_{DA} represents the strength of electronic interaction between the reactant and the product. The total reorganization energy λ_t is the sum of internal (λ_i), stemming from the difference in vibrational energy in the redox products, and solvent reorganization energy (λ_s; Table 1, footnote equation). Ferrocenes have been used as one electron redox system owing to its negligible internal reorganization (∼0.03 eV)[22] where the λ_i for the TBAPy within NU-1000 was reported to be ∼0.39 eV.[12] These values cannot account for the high λ_t (∼1 eV) required, especially, in low dielectric media such as toluene, 3-methyl pentane, and air to be comparable with the corresponding ΔG^0 values.

Though nonassociation of the charge-balancing counterions in a redox reaction can contribute to the reorganization energy by affecting the structure,[23] in our case, however, both of the redox products are held fixed as part of a relatively rigid mesoporous framework (with a low Fc/TBAPy loading ratio of 0.35 relative to the maximally possible crowded loading of 2.0) and thus should not significantly contribute to internal reorganization energy. Because the solvent reorganization energy (λ_s), in low-dielectric media, will not have much contribution to the λ_t; the framework must account for the required environmental response. A closer look at the **Fc@NU-1000** structure reveals that the Fc moieties anchored at the node are in close proximity to the polar hydroxy/aqua ligands at the Zr^{IV}-oxo cluster (Figure 1), which provides a water-like environment. Literature reports suggest that for a Fc/Fc^+ system, the λ_t in water can be taken as 1.0 eV (where λ_s ∼ 0.84–0.95 eV).[22] Polarization of the node bound hydroxy/aqua ligands by the ferrocenium ion thus accounts for the high reorganization energy required for quenching of a photoexcited TBAPy.

In conclusion, we have characterized the charge-transfer (CT) complex between photoexcited TBAPy linker and node anchored ferrocene moiety within a Zr-based metal–organic framework and probed the CT kinetics using femto- and pico-

DOI: 10.1021/jacs.7b13211
J. Am. Chem. Soc. 2018, 140, 2756–2760

second time-resolved spectroscopy. In these experiments, the CT products ($[NU\text{-}1000]^{\bullet-}/Fc^{+}$) are fixed in the mesoporous NU-1000 framework, which allowed a dielectric variation (examined here a range of $\epsilon_s = 1-37$) without the involvement of electrolyte based counterions. The dielectrics dependent CT kinetic data unambiguously indicate that the CT process involving a node bound redox partner that resides in close proximity to the polar $[Zr_6(\mu_3{-}O)_4(\mu_3{-}OH)_4(-OH)_4(-OH_2)_4]^{8+}$ node requires a large reorganization energy. This large reorganization energy is used to polarize the hydroxyl/aqua ligand at the node by the photoinduced charged product. We anticipate that the findings of this study will provide important consideration in the future design of MOF-based electrocatalytic and photoelectrochemical systems. For example, linkers that possess frontier molecular orbitals extended to the node-binding carboxy-phenyls might boost electronic tunneling but have to pay a reorganization energy penalty. Thus, a strategy that is capable of eliminating the node-bound polar hydroxyl/aqua ligands may become important.

■ ASSOCIATED CONTENT

Supporting Information

The Supporting Information is available free of charge on the ACS Publications website at DOI: 10.1021/jacs.7b13211.

Materials, instrumentation, and procedures; characterization; steady-state and time-resolved spectroscopic data (PDF)

■ AUTHOR INFORMATION

Corresponding Author

*pderia@siu.edu

ORCID

Jaehong Park: 0000-0002-0509-3934

Pravas Deria: 0000-0001-7998-4492

Present Address

§Department of Chemistry, Simpson College, 701 North C Street, Indianola, IA 50125, USA

Notes

The authors declare no competing financial interest.

■ ACKNOWLEDGMENTS

We thank SIUC for the startup support and IMAGE center (CHE0959568) for the SEM-EDS data. We also thank Advanced Coal & Energy Research Center for partial support through Energy Boost Seed Grant. P.D. acknowledges Ralph E. Powe Junior Faculty Enhancement Award, administered by ORAU. A.V.W. acknowledges NSF-REU fellowship (DMR-1461255). J.P. acknowledges JSPS KAKENHI Grant-in-Aid for Research Activity Start-up Grant Number 17H06791 and Dr. Yasunari Tamai and Kazuki Yoshitaka for their assistance on fs-TA measurements. We thank Dr. Chung-Wei Kung, Northwestern University, for DRIFTs data.

■ REFERENCES

(1) (a) Férey, G. *Chem. Soc. Rev.* **2008**, *37*, 191. (b) Yaghi, O. M.; O'Keeffe, M.; Ockwig, N. W.; Chae, H. K.; Eddaoudi, M.; Kim, J. *Nature* **2003**, *423*, 705.

(2) (a) Hu, Z.; Deibert, B. J.; Li, J. *Chem. Soc. Rev.* **2014**, *43*, 5815. (b) Kreno, L. E.; Leong, K.; Farha, O. K.; Allendorf, M.; Van Duyne, R. P.; Hupp, J. T. *Chem. Rev.* **2012**, *112*, 1105. (c) Cui, Y.; Yue, Y.; Qian, G.; Chen, B. *Chem. Rev.* **2012**, *112*, 1126. (d) Jin, S.; Son, H.-J.; Farha, O. K.; Wiederrecht, G. P.; Hupp, J. T. *J. Am. Chem. Soc.* **2013**, *135*, 955. (e) Kent, C. A.; Liu, D.; Ma, L.; Papanikolas, J. M.; Meyer, T. J.; Lin, W. *J. Am. Chem. Soc.* **2011**, *133*, 12940. (f) Kent, C. A.; Mehl, B. P.; Ma, L.; Papanikolas, J. M.; Meyer, T. J.; Lin, W. *J. Am. Chem. Soc.* **2010**, *132*, 12767. (g) So, M. C.; Jin, S.; Son, H.-J.; Wiederrecht, G. P.; Farha, O. K.; Hupp, J. T. *J. Am. Chem. Soc.* **2013**, *135*, 15698. (h) Son, H.-J.; Jin, S.; Patwardhan, S.; Wezenberg, S. J.; Jeong, N. C.; So, M.; Wilmer, C. E.; Sarjeant, A. A.; Schatz, G. C.; Snurr, R. Q.; Farha, O. K.; Wiederrecht, G. P.; Hupp, J. T. *J. Am. Chem. Soc.* **2013**, *135*, 862. (i) Wang, C.; Zhang, T.; Lin, W. *Chem. Rev.* **2012**, *112*, 1084. (j) Kung, C.-W.; Wang, T. C.; Mondloch, J. E.; Fairen-Jimenez, D.; Gardner, D. M.; Bury, W.; Klingsporn, J. M.; Barnes, J. C.; Van Duyne, R.; Stoddart, J. F.; Wasielewski, M. R.; Farha, O. K.; Hupp, J. T. *Chem. Mater.* **2013**, *25*, 5012.

(3) (a) Eddaoudi, M.; Kim, J.; Vodak, D.; Sudik, A.; Wachter, J.; O'Keeffe, M.; Yaghi, O. M. *Proc. Natl. Acad. Sci. U. S. A.* **2002**, *99*, 4900. (b) Furukawa, H.; Cordova, K. E.; O'Keeffe, M.; Yaghi, O. M. *Science* **2013**, *341*, 1230444. (c) O'Keeffe, M.; Yaghi, O. M. *Chem. Rev.* **2012**, *112*, 675. (d) Yaghi, O. M.; Li, H.; Davis, C.; Richardson, D.; Groy, T. L. *Acc. Chem. Res.* **1998**, *31*, 474.

(4) (a) Goswami, S.; Ma, L.; Martinson, A. B. F.; Wasielewski, M. R.; Farha, O. K.; Hupp, J. T. *ACS Appl. Mater. Interfaces* **2016**, *8*, 30863. (b) Williams, D. E.; Rietman, J. A.; Maier, J. M.; Tan, R.; Greytak, A. B.; Smith, M. D.; Krause, J. A.; Shustova, N. B. *J. Am. Chem. Soc.* **2014**, *136*, 11886. (c) Lin, J.; Hu, X.; Zhang, P.; Van Rynbach, A.; Beratan, D. N.; Kent, C. A.; Mehl, B. P.; Papanikolas, J. M.; Meyer, T. J.; Lin, W.; Skourtis, S. S.; Constantinou, M. *J. Phys. Chem. C* **2013**, *117*, 22250.

(5) (a) Ahrenholtz, S. R.; Epley, C. C.; Morris, A. J. *J. Am. Chem. Soc.* **2014**, *136*, 2464. (b) Narayan, T. C.; Miyakai, T.; Seki, S.; Dincă, M. *J. Am. Chem. Soc.* **2012**, *134*, 12932. (c) Kobayashi, Y.; Jacobs, B.; Allendorf, M. D.; Long, J. R. *Chem. Mater.* **2010**, *22*, 4120. (d) Talin, A. A.; Centrone, A.; Ford, A. C.; Foster, M. E.; Stavila, V.; Haney, P.; Kinney, R. A.; Szalai, V.; El Gabaly, F.; Yoon, H. P.; Léonard, F.; Allendorf, M. D. *Science* **2014**, *343*, 66. (e) Hod, I.; Sampson, M. D.; Deria, P.; Kubiak, C. P.; Farha, O. K.; Hupp, J. T. *ACS Catal.* **2015**, *5*, 6302. (f) Hod, I.; Bury, W.; Gardner, D. M.; Deria, P.; Roznyatovskiy, V.; Wasielewski, M. R.; Farha, O. K.; Hupp, J. T. *J. Phys. Chem. Lett.* **2015**, *6*, 586. (g) McGonigal, P. R.; Deria, P.; Hod, I.; Moghadam, P. Z.; Avestro, A.-J.; Horwitz, N. E.; Gibbs-Hall, I. C.; Blackburn, A. K.; Chen, D.; Botros, Y. Y.; Wasielewski, M. R.; Snurr, R. Q.; Hupp, J. T.; Farha, O. K.; Stoddart, J. F. *Proc. Natl. Acad. Sci. U. S. A.* **2015**, *112*, 11161.

(6) (a) Karagiaridi, O.; Lalonde, M. B.; Bury, W.; Sarjeant, A. A.; Farha, O. K.; Hupp, J. T. *J. Am. Chem. Soc.* **2012**, *134*, 18790. (b) McDonald, T. M.; D'Alessandro, D. M.; Krishna, R.; Long, J. R. *Chem. Sci.* **2011**, *2*, 2022. (c) Mondloch, J. E.; Bury, W.; Fairen-Jimenez, D.; Kwon, S.; DeMarco, E. J.; Weston, M. H.; Sarjeant, A. A.; Nguyen, S. T.; Stair, P. C.; Snurr, R. Q.; Farha, O. K.; Hupp, J. T. *J. Am. Chem. Soc.* **2013**, *135*, 10294. (d) Kim, M.; Cahill, J. F.; Fei, H.; Prather, K. A.; Cohen, S. M. *J. Am. Chem. Soc.* **2012**, *134*, 18082.

(7) (a) Deria, P.; Bury, W.; Hupp, J. T.; Farha, O. K. *Chem. Commun.* **2014**, *50*, 1965. (b) Deria, P.; Mondloch, J. E.; Karagiaridi, O.; Bury, W.; Hupp, J. T.; Farha, O. K. *Chem. Soc. Rev.* **2014**, *43*, 5896. (c) Deria, P.; Mondloch, J. E.; Tylianakis, E.; Ghosh, P.; Bury, W.; Snurr, R. Q.; Hupp, J. T.; Farha, O. K. *J. Am. Chem. Soc.* **2013**, *135*, 16801. (d) Deria, P.; Chung, Y. G.; Snurr, R. Q.; Hupp, J. T.; Farha, O. K. *Chem. Sci.* **2015**, *6*, 5172.

(8) (a) Scholes, G. D.; Fleming, G. R.; Olaya-Castro, A.; van Grondelle, R. *Nat. Chem.* **2011**, *3*, 763. (b) Barber, J.; Andersson, B. *Nature* **1994**, *370*, 31. (c) Cheng, Y.-C.; Fleming, G. R. *Annu. Rev. Phys. Chem.* **2009**, *60*, 241. (d) Mcdermott, G.; Prince, S. M.; Freer, A. A.; Hawthornthwaite-Lawless, A. M.; Papiz, M. Z.; Cogdell, R. J.; Isaacs, N. W. *Nature* **1995**, *374*, 517.

(9) (a) Wang, C.; Xie, Z.; deKrafft, K. E.; Lin, W. *J. Am. Chem. Soc.* **2011**, *133*, 13445. (b) Hod, I.; Deria, P.; Bury, W.; Mondloch, J. E.; Kung, C.-W.; So, M.; Sampson, M. D.; Peters, A. W.; Kubiak, C. P.; Farha, O. K.; Hupp, J. T. *Nat. Commun.* **2015**, *6*, 8304.

(10) (a) Diaz, R.; Orcajo, M. G.; Botas, J. A.; Calleja, G.; Palma, J. *Mater. Lett.* **2012**, *68*, 126. (b) Férey, G.; Millange, F.; Morcrette, M.;

DOI: 10.1021/jacs.7b13211
J. Am. Chem. Soc. 2018, 140, 2756−2760

Serre, C.; Doublet, M.-L.; Grenèche, J.-M.; Tarascon, J.-M. *Angew. Chem., Int. Ed.* **2007**, *46*, 3259.
(11) Huo, P.; Chen, T.; Hou, J.-L.; Yu, L.; Zhu, Q.-Y.; Dai, J. *Inorg. Chem.* **2016**, *55*, 6496.
(12) Patwardhan, S.; Schatz, G. C. *J. Phys. Chem. C* **2015**, *119*, 24238.
(13) Hod, I.; Farha, O. K.; Hupp, J. T. *Chem. Commun.* **2016**, *52*, 1705.
(14) (a) Cavka, J. H.; Jakobsen, S.; Olsbye, U.; Guillou, N.; Lamberti, C.; Bordiga, S.; Lillerud, K. P. *J. Am. Chem. Soc.* **2008**, *130*, 13850. (b) Chen, Y.; Hoang, T.; Ma, S. *Inorg. Chem.* **2012**, *51*, 12600. (c) Feng, D.; Gu, Z.-Y.; Li, J.-R.; Jiang, H.-L.; Wei, Z.; Zhou, H.-C. *Angew. Chem., Int. Ed.* **2012**, *51*, 10307. (d) Morris, W.; Volosskiy, B.; Demir, S.; Gándara, F.; McGrier, P. L.; Furukawa, H.; Cascio, D.; Stoddart, J. F.; Yaghi, O. M. *Inorg. Chem.* **2012**, *51*, 6443. (e) Jiang, H.-L.; Feng, D.; Wang, K.; Gu, Z.-Y.; Wei, Z.; Chen, Y.-P.; Zhou, H.-C. *J. Am. Chem. Soc.* **2013**, *135*, 13934. (f) Deria, P.; Gómez-Gualdrón, D. A.; Bury, W.; Schaef, H. T.; Wang, T. C.; Thallapally, P. K.; Sarjeant, A. A.; Snurr, R. Q.; Hupp, J. T.; Farha, O. K. *J. Am. Chem. Soc.* **2015**, *137*, 13183. (g) Kalidindi, S. B.; Nayak, S.; Briggs, M. E.; Jansat, S.; Katsoulidis, A. P.; Miller, G. J.; Warren, J. E.; Antypov, D.; Corà, F.; Slater, B.; Prestly, M. R.; Martí-Gastaldo, C.; Rosseinsky, M. J. *Angew. Chem., Int. Ed.* **2015**, *54*, 221. (h) Liu, T.-F.; Feng, D.; Chen, Y.-P.; Zou, L.; Bosch, M.; Yuan, S.; Wei, Z.; Fordham, S.; Wang, K.; Zhou, H.-C. *J. Am. Chem. Soc.* **2015**, *137*, 413. (i) Wang, T. C.; Bury, W.; Gómez-Gualdrón, D. A.; Vermeulen, N. A.; Mondloch, J. E.; Deria, P.; Zhang, K.; Moghadam, P. Z.; Sarjeant, A. A.; Snurr, R. Q.; Stoddart, J. F.; Hupp, J. T.; Farha, O. K. *J. Am. Chem. Soc.* **2015**, *137*, 3585. (j) Deria, P.; Gómez-Gualdrón, D. A.; Hod, I.; Snurr, R. Q.; Hupp, J. T.; Farha, O. K. *J. Am. Chem. Soc.* **2016**, *138*, 14449. (k) Deria, P.; Yu, J.; Balaraman, R. P.; Mashni, J.; White, S. N. *Chem. Commun.* **2016**, *52*, 13031.
(15) (a) Deria, P.; Bury, W.; Hod, I.; Kung, C.-W.; Karagiaridi, O.; Hupp, J. T.; Farha, O. K. *Inorg. Chem.* **2015**, *54*, 2185. (b) Deria, P.; Li, S.; Zhang, H.; Snurr, R. Q.; Hupp, J. T.; Farha, O. K. *Chem. Commun.* **2015**, *51*, 12478.
(16) Deria, P.; Yu, J.; Smith, T.; Balaraman, R. P. *J. Am. Chem. Soc.* **2017**, *139*, 5973.
(17) The effective quenching radius of the installed ferrocene defines the effective hopping efficiency of the linker-based exciton and is known to a function of MOF topology (see ref 2h).
(18) Marcus, R. A. *J. Chem. Phys.* **1965**, *43*, 679.
(19) (a) Gray, H. B.; Winkler, J. R. *Proc. Natl. Acad. Sci. U. S. A.* **2005**, *102*, 3534. (b) Winkler, J. R.; Gray, H. B. *J. Am. Chem. Soc.* **2014**, *136*, 2930.
(20) Weller, A. *Z. Phys. Chem.* **1982**, *133*, 93.
(21) Coropceanu, V.; Cornil, J.; da Silva Filho, D. A.; Olivier, Y.; Silbey, R.; Brédas, J.-L *Chem. Rev.* **2007**, *107*, 926.
(22) (a) Chidsey, C. E. D. *Science* **1991**, *251*, 919. (b) Smalley, J. F.; Feldberg, S. W.; Chidsey, C. E. D.; Linford, M. R.; Newton, M. D.; Liu, Y.-P. *J. Phys. Chem.* **1995**, *99*, 13141.
(23) Orlowski, G. A.; Chowdhury, S.; Kraatz, H.-B. *Langmuir* **2007**, *23*, 12765.

DOI: 10.1021/jacs.7b13211
J. Am. Chem. Soc. 2018, 140, 2756−2760